

Quantum transport in honeycomb lattice ribbons with zigzag edges: A theoretical study

Santanu K. Maiti^{1,2,1}

¹*Theoretical Condensed Matter Physics Division, Saha Institute of Nuclear Physics,
1/AF, Bidhannagar, Kolkata-700 064, India*

²*Department of Physics, Narasinha Dutt College, 129 Belilious Road, Howrah-711 101, India*

Abstract

We explore electron transport properties in honeycomb lattice ribbons with zigzag edges coupled to two semi-infinite one-dimensional metallic electrodes. The calculations are based on the tight-binding model and the Green's function method, which numerically compute the conductance-energy and current-voltage characteristics as functions of the lengths and widths of the ribbons. Our numerical results predict that for such a ribbon an energy gap always appears in the conductance spectrum across the energy $E = 0$. With the increase of the size of the ribbon, the gap gradually decreases but it never vanishes. This clearly manifests that a honeycomb lattice ribbon with zigzag edges always exhibits the semiconducting behavior, and it becomes much more clearly visible from our presented current-voltage characteristics.

PACS No.: 73.63.-b; 73.63.Rt.

Keywords: Honeycomb lattice ribbon; Zigzag edges; Conductance; I - V characteristic.

¹**Corresponding Author:** Santanu K. Maiti
Electronic mail: santanu.maiti@saha.ac.in

1 Introduction

The electronic transport in graphene nanoribbons has opened up new challenges in nanoelectronics. A graphene nanoribbon (GNR) is a monolayer of carbon atoms arranged in a two-dimensional honeycomb lattice structure¹⁻⁴ and can be regarded as the basic building blocks for graphitic materials. Graphene based materials have potential applications in several branch of nanoelectronics and due to their special electronic and physical properties they exhibit several novel properties like high carrier mobility,³ unconventional quantum Hall effect⁵ and many others. The high carrier mobility in graphene demonstrates the idea for fabrication of high speed switching devices those have widespread applications in different fields. Recently GNRs are also used extensively in designing field-effect transistors and this idea has been predicted in some recent nice papers.⁶⁻⁸ It has many potential applications and provides a huge interest in the community of nanoelectronics device research. Not only that, GNRs can be used to construct MOSFETs which perform much better than conventional Si MOSFETs. In other experiment⁹ it has been proposed that a narrow strip of graphene, the so-called a graphene nanoribbon, exhibits semiconducting behavior due to its edge effects, unlike carbon nanotubes of larger sizes which are mixtures of both metallic and semiconducting materials. The reason is that, in a narrow graphene sheet a band gap appears across the energy $E = 0$, while the gap gradually disappears with the increase of the size of the ribbon. It reveals a transformation from the semiconducting to the metallic material. This phenomenon has been studied in detail in a very recent theoretical work by the same author of this paper.¹⁰ The situation becomes quite different for the case of honeycomb lattice ribbons with zigzag edges. Our study predicts that for a ribbon with zigzag edges always there exists an energy gap in the conductance spectrum across the energy $E = 0$. The gap gradually decreases with the increase of the size of the ribbon (as expected), but it never vanishes even for much larger ribbons. This clearly reveals that a honeycomb lattice ribbon with zigzag edges always exhibits the semiconducting behavior, unlike the lattice ribbons with armchair edges where both the semiconducting and the metallic phases are observed by tuning the size of a ribbon. All these edge effects in graphene ribbons provide many key informations in designing nanoelectronic devices.

The aim of the present paper is to provide a qual-

itative study of electron transport in honeycomb lattice ribbons with zigzag edges attached to two semi-infinite one-dimensional metallic electrodes (see Fig. 1). The theoretical description of electron transport in a bridge system has been developed based on the pioneering work of Aviram and Ratner.¹¹ Later, many significant experiments¹²⁻¹³ have been done in several bridge systems to understand the basic mechanisms underlying the electron transport. Though in literature many theoretical¹⁴⁻²⁵ as well as experimental papers¹²⁻¹³ on electron transport are available, yet lot of controversies are still present between the theory and experiment even today. Several controlling factors are there which can regulate the electron transport in a conducting bridge significantly, and all these factors have to be taken into account properly to understand the transport mechanism. For our illustrative purposes, here we mention some of these issues.

- (i) The geometry of the conducting material between the two electrodes itself is an important issue to control the electron transmission which has been described quite elaborately by Ernzerhof *et al.*²⁶ through some model calculations.
- (ii) The coupling of the bridging material to the electrodes significantly controls the current amplitude across any bridge system.²⁷
- (iii) The quantum interference effect²⁷⁻³¹ of electron waves passing through different arms of the bridging material becomes the most significant issue.
- (iv) The dynamical fluctuation in the small-scale devices is another important factor which plays an active role and can be manifested through the measurement of *shot noise*,³²⁻³³ a direct consequence of the quantization of charge.

In addition to these, several other factors of the Hamiltonian that describe a system also provide important effects in the determination of the current across a bridge system.

Here we adopt a simple tight-binding model to describe the system and all the calculations are performed numerically. We narrate the conductance-energy and current-voltage characteristics as functions of the lengths and widths of ribbons. Our results clearly predicts that a honeycomb lattice ribbon with zigzag edges always shows the semiconducting nature irrespective of its length and width.

The paper is arranged in this way. Following the introduction (Section 1), in Section 2, we present the model and the theoretical formulations for our calculations. Section 3 discusses the significant re-

sults, and the summary of this work is available in Section 4.

2 Model and synopsis of the theoretical background

Let us start with Fig. 1, where a honeycomb lattice ribbon with zigzag edges is attached to two semi-infinite one-dimensional metallic electrodes, viz, source and drain. As the electron transport properties are significantly influenced by the quan-

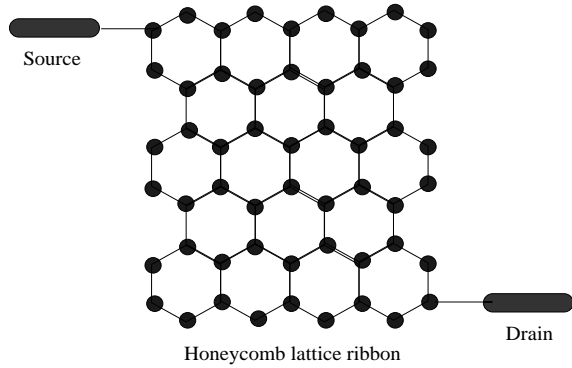


Figure 1: (Color online). Schematic view of a honeycomb lattice ribbon with zigzag edges attached to two semi-infinite one-dimensional metallic electrodes, viz, source and drain. Filled circles correspond to the position of the atomic sites.

tum interference effects, throughout the study, we contact the electrodes at the two extreme ends of nanoribbons (see Fig. 1) to make these interference effects uniform.

Calculation of the conductance:

We use the Landauer conductance formula^{34–35} to calculate the conductance g of the ribbon. At very low temperature and bias voltage it (g) can be presented in the form,

$$g = \frac{2e^2}{h} T \quad (1)$$

where T gives the transmission probability of an electron in the ribbon which can be expressed in terms of the Green's function of the ribbon and its coupling to the two electrodes by the relation,^{34–35}

$$T = \text{Tr} [\Gamma_S G_{rib}^r \Gamma_D G_{rib}^a] \quad (2)$$

where G_{rib}^r and G_{rib}^a are respectively the retarded and advanced Green's functions of the ribbon including the effects of the electrodes. The parameters Γ_S and Γ_D describe the coupling of the ribbon

to the source and drain respectively, and they can be defined in terms of their self-energies. For the complete system i.e., the ribbon, source and drain, the Green's function is defined as,

$$G = (\mathcal{E} - H)^{-1} \quad (3)$$

where $\mathcal{E} = E + i\delta$. E is the injecting energy of the source electron and δ gives an infinitesimal imaginary part to \mathcal{E} . To Evaluate this Green's function, the inversion of an infinite matrix is needed since the complete system consists of the finite ribbon and the two semi-infinite electrodes. However, the entire system can be partitioned into sub-matrices corresponding to the individual sub-systems and the Green's function for the ribbon can be effectively written as,

$$G_{rib} = (\mathcal{E} - H_{rib} - \Sigma_S - \Sigma_D)^{-1} \quad (4)$$

where H_{rib} is the Hamiltonian of the ribbon which can be written in the tight-binding model within the non-interacting picture like,

$$H_{rib} = \sum_i \epsilon_i c_i^\dagger c_i + \sum_{\langle ij \rangle} t (c_i^\dagger c_j + c_j^\dagger c_i) \quad (5)$$

In the above Hamiltonian (H_{rib}), ϵ_i 's are the site energies, c_i^\dagger (c_i) is the creation (annihilation) operator of an electron at the site i and t is the nearest-neighbor hopping integral. A similar kind of tight-binding Hamiltonian is also used to describe the two semi-infinite one-dimensional perfect electrodes where the Hamiltonian is parametrized by constant on-site potential ϵ_0 and nearest-neighbor hopping integral t_0 . In Eq. 4, $\Sigma_S = h_{S-rib}^\dagger g_S h_{S-rib}$ and $\Sigma_D = h_{D-rib}^\dagger g_D h_{D-rib}$ are the self-energy operators due to the two electrodes, where g_S and g_D correspond to the Green's functions of the source and drain respectively. h_{S-rib} and h_{D-rib} are the coupling matrices and they will be non-zero only for the adjacent points of the ribbon, and the electrodes respectively. The matrices Γ_S and Γ_D can be calculated through the expression,

$$\Gamma_{S(D)} = i \left[\Sigma_{S(D)}^r - \Sigma_{S(D)}^a \right] \quad (6)$$

where $\Sigma_{S(D)}^r$ and $\Sigma_{S(D)}^a$ are the retarded and advanced self-energies respectively, and they are conjugate with each other. These self-energies can be written as,³⁶

$$\Sigma_{S(D)}^r = \Lambda_{S(D)} - i\Delta_{S(D)} \quad (7)$$

where $\Lambda_{S(D)}$ are the real parts of the self-energies which correspond to the shift of the energy eigenvalues of the ribbon and the imaginary parts $\Delta_{S(D)}$ of

the self-energies represent the broadening of these energy levels. Since this broadening is much larger than the thermal broadening, we restrict our all calculations only at absolute zero temperature. All the information about the ribbon-to-electrode coupling are included into these two self-energies.

Calculation of the current:

The current passing across the ribbon can be depicted as a single-electron scattering process between the two reservoirs of charge carriers. The current I can be computed as a function of the applied bias voltage V through the relation,³⁴

$$I(V) = \frac{2e}{h} \int_{E_F - eV/2}^{E_F + eV/2} T(E) dE \quad (8)$$

where E_F is the equilibrium Fermi energy. Here we make a realistic assumption that the entire voltage is dropped across the ribbon-electrode interfaces, and it is examined that under such an assumption the I - V characteristics do not change their qualitative features. This assumption is based on the fact that, the electric field inside the ribbon especially for narrow ribbons seems to have a minimal effect on the conductance-voltage characteristics. On the other hand, for quite larger ribbons and high bias voltages the electric field inside the ribbon may play a more significant role depending on the internal structure and size of the ribbon,³⁶ but the effect becomes too small.

3 Numerical results and discussion

To have a better insight in the present problem i.e., the dependence of the electron transport on the lengths and widths of ribbons, we focus our attention only on the perfect systems rather than any disordered one. To get these perfect systems we fix the on-site energies $\epsilon_i = 0$ for all the sites i of the honeycomb lattice ribbons. The values of the other parameters are taken as follow. The nearest-neighbor hopping integral t in the ribbon is set to 1, the on-site energy ϵ_0 and the hopping integral t_0 for the two electrodes are fixed to 0 and 1 respectively. The parameters τ_S and τ_D are set as 0.75, where they correspond to the hopping strengths of the ribbon to the source and drain respectively. In addition to these, to describe the size of a ribbon we introduce two other parameters N and M where

they correspond to the width and length of the ribbon respectively. Thus, for example, a nanoribbon with $N = 1$ and $M = 3$ represents a linear chain of three hexagons. Hence the parameter M determines the total number of hexagons in a single chain. Following this rule, a nanoribbon with $N = 3$ and $M = 4$ corresponds to three linear chains at-

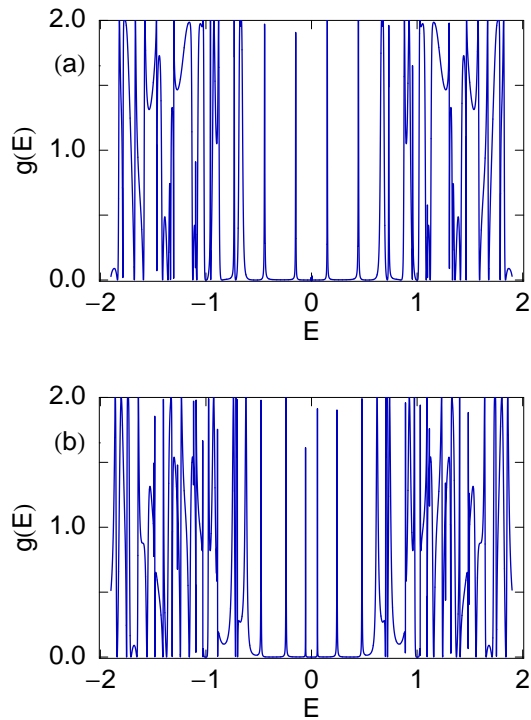


Figure 2: (Color online). Conductance g as a function of the energy E for some lattice ribbons with fixed width $N = 3$ and varying lengths where (a) $M = 6$ and (b) $M = 8$.

tached side by side (see Fig. 1) where each chain contains four hexagons. For simplicity, throughout our study we set the Fermi energy $E_F = 0$ and choose the units where $c = e = h = 1$.

Let us begin our discussion with the variation of the conductance g as a function of the energy E . In Fig. 2 we plot the conductance-energy characteristics for some typical lattice ribbons with fixed width $N = 3$ and varying lengths where (a) and (b) correspond to the lengths $M = 6$ and 8 respectively. The sharp resonant peaks in the conductance spectra are observed almost for all energies, while for some other energies either the conductance g gets much small value or drops to zero. At the resonances the conductance gets the value 2, and therefore, the transmission probability T becomes unity

since the relation $g = 2T$ follows from the Landauer conductance formula, Eq. 1, with $e = h = 1$. Now the reduction of the transmission probability ($T < 1$) for some particular energies can be explained by considering the quantum interference effects of the electronic waves passing through the different arms of the ribbon. The interpretation is as follow. During the motion of the electrons from

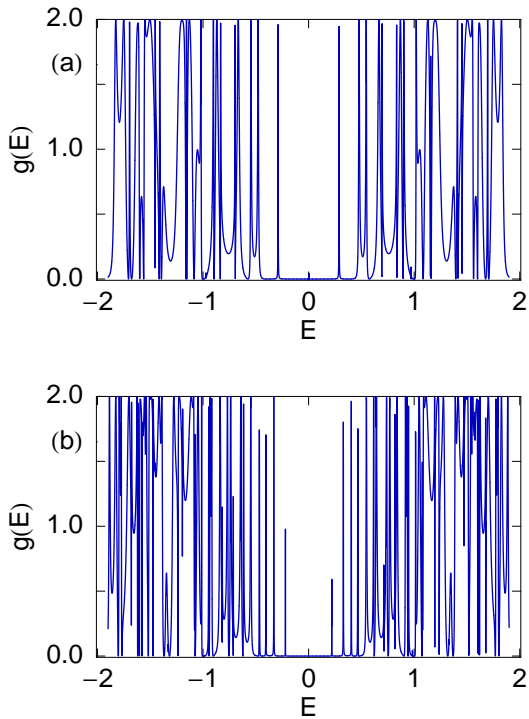


Figure 3: (Color online). Conductance g as a function of the energy E for some lattice ribbons with fixed length $M = 4$ and varying widths where (a) $N = 5$ and (b) $N = 10$.

the source to drain through the lattice ribbon, the electron waves propagating along the different possible pathways can get a phase shift among themselves, according to the result of quantum interference. Therefore, the probability amplitude of getting an electron across the ribbon either becomes strengthened or weakened. This causes the transmittance cancellations and provides anti-resonances in the conductance spectrum. Thus it can be emphasized that the electron transmission is strongly affected by the quantum interference effects, and hence the ribbon to electrode interface structure. Now all these resonant peaks are associated with the energy eigenvalues of the ribbon, and accordingly, we can say that the conductance spectrum

manifests itself the electronic structure of the ribbon. Due to the large number of energy levels, associated with the size of the ribbons, the resonant peaks almost overlap with each other and form quasi-continuous spectra in the g - E characteristics. The most significant feature observed from the spec-

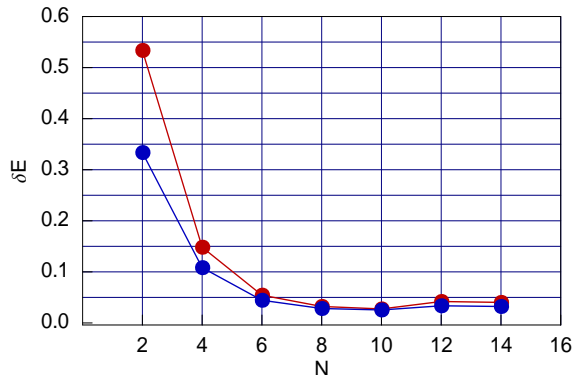


Figure 4: (Color online). Variation of the central energy gap δE as a function of the width N for some lattice ribbons with fixed lengths M . The red and blue curves correspond to $M = 2$ and 4 respectively.

tra, given in Fig. 2, is that a central energy gap (δE) appears across the energy $E = 0$. With the increase of the length of the ribbon some more resonant peaks appear around $E = 0$, and accordingly, the gap decreases which is clearly observed from Figs. 2(a) and (b). Thus for a fixed width, the central gap can be controlled by tuning the length of the ribbon.

In the same fashion, to characterize the dependence of the electron transport on the widths of the ribbons for a fixed length, in Fig. 3 we plot the results for some typical lattice ribbons considering the length $M = 4$. The spectra shown in Figs. 3(a) and (b) correspond to the ribbons with widths $N = 5$ and 10 respectively. Quite similar to the above case, here also a gap appears across $E = 0$ and it decreases with the increase of the width of the ribbon though the reduction is much small. Thus from the results described in Figs. 2 and 3 we can emphasize that the width of the central energy gap always decreases with the increase of the size (length and width) of the ribbon.

To illustrate the dependence of the gap δE with other system sizes, in Fig. 4, we display the variation of δE as a function of the width N for some typical lattice ribbons with fixed lengths. The red and blue curves correspond to the lengths $M = 2$ and 4 respectively. Quite interestingly we see that,

the gap δE gradually decreases with the increase of the width N , and beyond a certain value of N , the rate of decrease of this gap becomes much small and eventually it (δE) becomes almost a constant. Quite similar feature is also observed if we plot the variation of the energy gap as a function of the length M keeping the width N as a constant, and due to the obvious reason we do not plot these results further in the present description. These re-

sults provide us an important signature which concern with the variation of the energy gap by tuning the size of the ribbon, and we can emphasize that a honeycomb lattice ribbon with zigzag edges always exhibits the semiconducting (finite energy gap) behavior.

factor 2, since the relation $g = 2T$ holds from the Landauer conductance formula (Eq. 1). As an illustration, in Fig. 5, we present the current-voltage (I - V) characteristics for some lattice ribbons with fixed width $N = 3$ and varying lengths where (a) and (b) correspond to the lengths $M = 3$ and 6 respectively. In the same footing, in Fig. 6, we plot the variation of the current I as a function of the bias voltage V for some typical lattice ribbons keep-

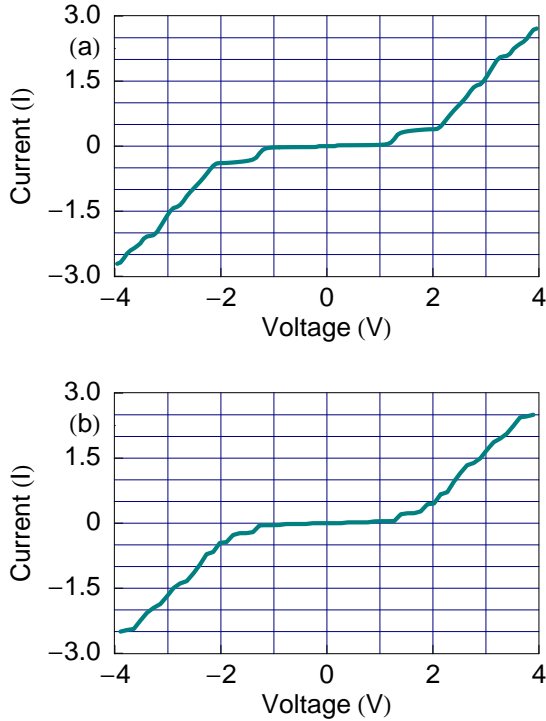


Figure 5: (Color online). Current I as a function of the bias voltage V for some lattice ribbons with fixed width $N = 3$ and varying lengths where (a) $M = 3$ and (b) $M = 6$.

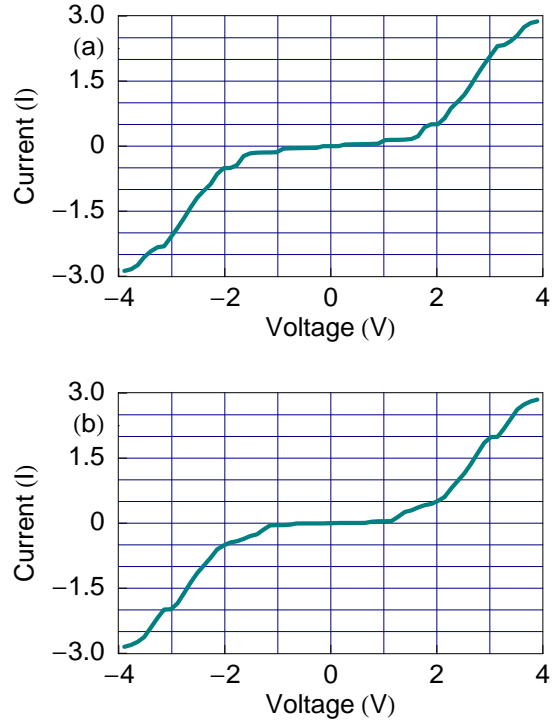


Figure 6: (Color online). Current I as a function of the bias voltage V for some lattice ribbons with fixed length $M = 4$ and varying widths where (a) $N = 2$ and (b) $N = 3$.

sults provide us an important signature which concern with the variation of the energy gap by tuning the size of the ribbon, and we can emphasize that a honeycomb lattice ribbon with zigzag edges always exhibits the semiconducting (finite energy gap) behavior.

All these basic features of electron transfer can be much more clearly explained from our investigation of the current-voltage (I - V) characteristics rather than the conductance-energy spectra. The current I is determined from the integration procedure of the transmission function (T) (see Eq. 8), where the function T varies exactly similar to the conductance spectra, differ only in magnitude by a

ing the length as fixed ($M = 4$) and vary the widths, where (a) and (b) represent the ribbons with widths $N = 2$ and 3 respectively. The sharpness in the I - V characteristics and the current amplitude solely depend on the coupling strengths of the ribbon to the side attached electrodes, viz, source and drain. It is observed that, in the limit of weak coupling, defined by the condition $\tau_{S(D)} \ll t$, current shows staircase like structure with sharp steps. While, in the strong coupling limit, described by the condition $\tau_{S(D)} \sim t$, current varies quite continuously with the bias voltage V and achieves large current amplitude compared to the weak-coupling limit. All these coupling effects have already been explained

in many theoretical as well as experimental papers in the literature. The key feature observed from these I - V characteristics is that for all such ribbons the electron starts to conduct beyond some finite bias voltage, the so-called threshold bias voltage V_{th} , and it decreases very slowly with the change of the size of the ribbon. Our study reveals that the threshold bias voltage never drops to zero, even for much larger systems, and accordingly, we can predict that a honeycomb lattice ribbon with zigzag edges exhibits only the semiconducting behavior.

4 Concluding remarks

To summarize, we have addressed electron transport properties in honeycomb lattice ribbons with zigzag edges attached to two semi-infinite one-dimensional metallic electrodes within the tight-binding framework. We have numerically computed the conductance-energy and current-voltage characteristics concerning the dependence on the lengths and widths of the ribbons. The results have predicted that for such ribbons i.e., ribbons with zigzag edges a central energy gap always exists across the energy $E = 0$ in the conductance spectrum. The gap decreases gradually with the increase of the size of the ribbon but it never vanishes. This phenomenon clearly manifests that a honeycomb lattice ribbon with zigzag edges always shows semiconducting nature, unlike the lattice ribbons with armchair edges where both the semiconducting and the metallic phases are observed by controlling the size of the ribbon. This semiconducting behavior of the lattice ribbons with zigzag edges has been much more clearly addressed from our presented current-voltage characteristics. It has been observed that the current starts to appear beyond some finite bias voltage i.e., the threshold bias voltage V_{th} has a non-zero value. This V_{th} doesn't change appreciably with the increase of the size of the ribbon and we have also examined that the threshold bias voltage never reduces to zero even for much larger systems, which predicts the semiconducting nature only.

This is our first step to describe how the electron transport properties in honeycomb lattice ribbons with zigzag edges depends on the size of the ribbons. We have made several realistic assumptions by ignoring the effects of the electron-electron correlation, disorder, interaction with a substrate, temperature, finite width of the electrodes, boundary of the ribbons, etc. Here we discuss very briefly about these approximations. The inclusion of the electron-electron correlation in the present model

is a major challenge to us, since over the last few years people have studied a lot to incorporate this effect, but no such proper theory has yet been developed. In this work, we have presented all the results only for the ordered systems. But in real samples, the presence of impurities will affect the electronic structure and hence the transport properties. Beside these, in experiments, the graphene nanoribbon is deposited on an insulating substrate which has also not been included in our present study, and, it has been observed from first-principles calculations that the effect of the substrate is too weak.³⁷ The effect of the temperature has already been pointed out earlier, and, it has been examined that the presented results will not change significantly even at finite temperature, since the broadening of the energy levels of the ribbon due to its coupling with the electrodes will be much larger than that of the thermal broadening.³⁴ The other important assumption is that here we have chosen the linear chains instead of wider leads, since we are mainly interested about the basic physics of the ribbon. Though the results presented here change with the increase of the thickness of the leads, but all the basic features remain quite invariant. The effect of the boundary is also an important issue in this context. Here we have considered only the perfect geometry of the nanoribbons. Several interesting features will be observed for the nanoconstrictions with different shapes³⁸ like, square-shaped, wedge-shaped nanoconstrictions, etc. Finally, we would like to say that we need further study in such systems by incorporating all these effects.

References

- [1] V. V. Cheianov, V. Fal'ko, and B. L. Altshuler, *Science* 315, 1252 (2007).
- [2] J. B. Pendry, *Science* 315, 1226 (2007).
- [3] A. K. Geim and K. S. Novoselov, *Nat. Mater.* 6, 183 (2007).
- [4] C. Berger, Z. Song, X. Li, X. Wu, N. Brown, C. Naud, D. Mayou, T. Li, J. Hass, A. N. Marchenkov, E. H. Corrad, P. N. First, and W. A. de Heer, *Science* 312, 1191 (2006).
- [5] Y. Zhang, Y. Tan, H. L. Stormer, and P. Kim, *Nature* 438, 201 (2005).
- [6] Y. Ouyang, Y. Yoon, J. K. Fodor, and J. Guo, *Appl. Phys. Lett.* 89, 203107 (2006).

- [7] Q. Yan, B. Huang, J. Yu, F. Zheng, J. Zang, J. Wu, B.-L. Gu, F. Liu, and W. Duan, *Nano Lett.* 7, 1469 (2007).
- [8] D. A. Areshkin and C. T. White, *Nano Lett.* 7, 3253 (2007).
- [9] X. Li, X. Wang, L. Zhang, S. Lee, and H. Dai, *Science* 319, 1229 (2008).
- [10] S. K. Maiti, *Solid State Commun.* 149, 973 (2009).
- [11] A. Aviram and M. Ratner, *Chem. Phys. Lett.* 29, 277 (1974).
- [12] K. S. Novoselov, A. K. Geim, S. V. Morozov, D. Jiang, M. I. Kastnelson, I. V. Grigorieva, S. V. Dubonos, and A. A. Firsov, *Nature (London)* 438, 197 (2005).
- [13] K. S. Novoselov, A. K. Geim, S. M. Morozov, D. Jiang, Y. Zhang, S. V. Dubonos, I. V. Grigorieva, and A. A. Firsov, *Science* 306, 666 (2004).
- [14] K. Wakabayashi, *Phys. Rev. B* 64, 125428 (2001).
- [15] K. Wakabayashi, M. Fujita, H. Ajiki, and M. Sigrist, *Phys. Rev. B* 59, 8271 (1999).
- [16] K. Wakabayashi, *J. Phys. Chem. Solid.* 69, 1162 (2008).
- [17] K. Wakabayashi and M. Sigrist, *Synth. Metal.* 121, 1231 (2001).
- [18] G. Liang, N. Neophytou, M. S. Lundstrom, and D. E. Nikonov, *Nano Lett.* 8, 1819 (2008).
- [19] O. Hod, J. E. Peralta, and G. E. Scuseria, *Phys. Rev. B* 76, 233401 (2007).
- [20] A. Cresti, G. Grosso, and G. P. Parravicini, *Phys. Rev. B* 76, 205433 (2007).
- [21] E. Cuansing and J. S. Wang, arXiv:0810.2181.
- [22] S. M. Cronenwett, T. H. Oosterkamp, and L. P. Kouwenhoven, *Science* 281, 5 (1998).
- [23] A. W. Holleitner, R. H. Blick, A. K. Huttel, K. Eber, and J. P. Kotthaus, *Science* 297, 70 (2002).
- [24] P. A. Orellana, M. L. Ladron de Guevara, M. Pacheco, and A. Latge, *Phys. Rev. B* 68, 195321 (2003).
- [25] P. A. Orellana, F. Dominguez-Adame, I. Gomez, and M. L. Ladron de Guevara, *Phys. Rev. B* 67, 085321 (2003).
- [26] M. Ernzerhof, M. Zhuang, and P. Rocheleau, *J. Chem. Phys.* 123, 134704 (2005).
- [27] R. Baer and D. Neuhauser, *Chem. Phys.* 281, 353 (2002).
- [28] R. Baer and D. Neuhauser, *J. Am. Chem. Soc.* 124, 4200 (2002).
- [29] D. Walter, D. Neuhauser, and R. Baer, *Chem. Phys.* 299, 139 (2004).
- [30] K. Tagami, L. Wang, and M. Tsukada, *Nano Lett.* 4, 209 (2004).
- [31] K. Walczak, *Cent. Eur. J. Chem.* 2, 524 (2004).
- [32] Y. M. Blanter and M. Buttiker, *Phys. Rep.* 336, 1 (2000).
- [33] K. Walczak, *Phys. Stat. Sol. (b)* 241, 2555 (2004).
- [34] S. Datta, *Electronic transport in mesoscopic systems*, Cambridge University Press, Cambridge (1997).
- [35] M. B. Nardelli, *Phys. Rev. B* 60, 7828 (1999).
- [36] W. Tian, S. Datta, S. Hong, R. Reifenberger, J. I. Henderson, and C. I. Kubiak, *J. Chem. Phys.* 109, 2874 (1998).
- [37] B. Obradovic, R. Kotlyar, F. Heinz, P. Matagne, T. Rakshit, M. D. Giles, M. A. Stettler, and D. E. Nikonov, *Appl. Phys. Lett.* 88, 142102 (2006).
- [38] F. Munoz-Rojas, D. Jacob, J. Fernandez-Rossier, and J. J. Palacios, *Phys. Rev. B* 74, 195417 (2006).